Bioorganic Chemistry 88 (2019) 102916

Contents lists available at ScienceDirect

Bioorganic Chemistry

journal homepage: www.elsevier.com/locate/bioorg

Synthesis and anti-tumor activity of [1,4] dioxino [2,3-f] quinazoline derivatives as dual inhibitors of c-Met and VEGFR-2

Dengshuai Wei[a], Haoru Fan[a], Kun Zheng[b], Xuemei Qin[c], Leifu Yang[b], Yajuan Yang[b], Ye Duan[b], Qiang Zhang[b], Chengchu Zeng[a], Liming Hu[a,*]

[a] College of Life Science and Bioengineering & Beijing Key Laboratory of Environmental and Oncology, Beijing University of Technology, Beijing 100124, China
[b] Beijing Scitech-MQ Pharmaceuticals Limited, Beijing 101320, China
[c] Guangxi Key Laboratory Cultivation Base for Polysaccharide Materials and Modifications, School of Marine Science and Biotechnology, Guangxi University for Nationalities, Nanning 530008, China

ARTICLE INFO

Keywords:
c-Met
VEGFR-2
Quinazoline derivatives
Antiproliferative effect
Cancer therapy

ABSTRACT

Both c-Met and VEGFR-2 were important targets for cancer therapies. In order to develop reversible and non-covalent c-Met and VEGFR-2 dual inhibitors, a series of [1,4]dioxino[2,3-*f*]quinazoline derivatives were designed and synthesized. The enzyme assay demonstrated that most target compounds had inhibition potency on both c-Met and VEGFR-2 with IC_{50} values in nanomolar range especially compounds **7m** and **7k**. Based on further cell proliferation assay *in vitro*, compound **7k** showed significantly anti-tumor activity *in vivo* on a hepatocellular carcinoma (MHCC97H cells) xenograft mouse model. We docked the compound **7m** with c-Met and VEGFR-2 kinases, and interpreted the SAR of these analogues. All results indicated that the target compounds were dual inhibitors of c-Met and VEGFR-2 kinases that held promising potential in cancer therapy.

1. Introduction

c-Mesenchymal epithelial transition factor(c-Met) and vascular endothelial growth factor receptor two (VEGFR-2) tyrosine kinases play key roles in signaling pathways that are exploited during the oncogenic process, including regulation of cell proliferation, invasion, angiogenesis, and cancer stem cell regulation [1]. While some c-Met or VEGFR-2 signal-targeted drugs have been approved for clinical application, their efficiency is limited due to the drug resistance as well as possible relevant toxicities. To overcome these limitations, anti-tumor therapies based on dual targets c-Met and VEGFR-2 tyrosine kinase inhibitors have become one of the hot spots of clinical treatments in cancer therapy. In recent years, Cabozantinib, Foretinib and other potential compounds are under investigation as dual c-Met and VEGFR-2 small molecular inhibitors [2–4]. With the great efforts to design dual target small molecule inhibitors, novel anticancer agents will emerge to affect both c-Met and VEGFR-2 in higher potency and selectivity.

c-Met, a tyrosine kinase for hepatocyte growth factor/scatter factor (HGF), is widely over-expressed in human tumors. Binding of HGF to c-Met induces phosphorylation of tyrosine residues on c-Met and activates its downstream signaling pathway [5,6]. c-Met has been proved to be regularly amplified or over-expressed in many kinds of cancers, including brain, colorectal, lung, neck, gastric, head and stomach cancers. Importantly, abnormal c-Met activation is observed frequently in many human solid tumors and hematological malignancies are related to poor clinical outcomes [7–9]. So, c-Met exhibits high potential as a target for human cancer therapy.

VEGFR-2, a tyrosine kinase receptor expressed in endothelial cells, binds to VEGF to induce a conformational change in VEGFR and followed by receptor dimerization and phosphorylation of tyrosine residues. The conformation changes to direct the signal to the downstream. The downstream signaling pathways include Ras (retrovirus associated DNA sequences)/Raf (rapidly accelerated fibrosarcoma)/MAPK (mitogenactivated protein kinase) and PI3K (phosphatidyl inositol-3 kinase)/Akt (protein kinase B) pathway [10]. After several of these pathways being activated, the occurrence of the tumor becomes possible. Inhibition of VEGFR-2 has been considered as an effective approach to the blockade of tumor growth [11].

c-Met has been shown to cooperate synergistically with VEGFR-2, resulting in promoting angiogenesis of development and progression of various human cancers [12–14]. Therefore, molecules that simultaneously inhibit c-Met and VEGFR-2 may be more reasonable to either c-Met selective or VEGFR-2 selective inhibitor as they can disturb multiple signaling pathways involved in tumor angiogenesis, proliferation, and metastasis [2,3,15,16].

Cabozantinib (**I**), an approved drug for the treatment of medullary

* Corresponding author.
E-mail address: huliming@bjut.edu.cn (L. Hu).

https://doi.org/10.1016/j.bioorg.2019.04.010
Received 11 January 2019; Received in revised form 4 April 2019; Accepted 6 April 2019
Available online 08 April 2019

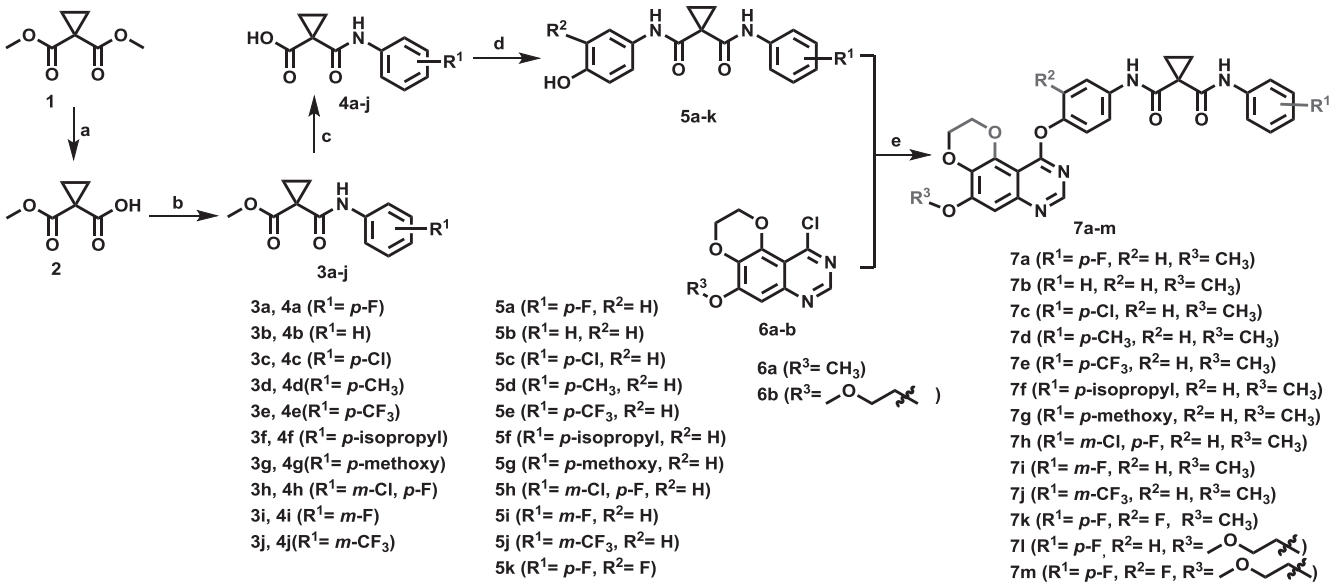

Scheme 1. Synthetic routes for a series of dual c-Met and VEGFR-2 inhibitors. Reagents and conditions: (a) LiOH, MeOH/H_2O, rt. 1 h; (b) EDC, HOBt, DCM, aniline or substituted aniline; (c) LiOH, MeOH/H_2O, rt.; (d) EDC, DMA, substituted or unsubstituted 4-aminophenol; (e) K_2CO_3, isopropanol.

thyroid cancer, a second line treatment for renal cell carcinoma and advanced hepatocellular carcinoma (HCC) who has received prior Sorafenib, is a highly potent c-Met and VEGFR-2 inhibitor [17]. Foretinib (**II**) is an experimental drug candidate for the treatment of cancer, designed to target the receptor tyrosine kinases c-Met and VEGFR-2 both of which have been implicated in the development, progression, and spread of cancer [18]. In our previous research, a series of dihydro [1,4]dioxino[2,3-f]quinazoline derivatives are synthesized as EGFR inhibitors, indicating that the core structure of dihydro[1,4]dioxino [2,3-f]quinazoline has potential use for tyrosine kinase inhibitors [19]. The cyclopropane-1,1-dicarboxamide moiety of compound **I** and **II** might be important for the high inhibitory activity to c-Met and VEGFR-2.

Based on the assumption, we designed and synthesized compound **7a**, which was a hybrid structure containing both the cyclopropane-1,1-dicarboxamide moiety of Cabozantinib or Foretinib and the dihydro [1,4]dioxino[2,3-f] quinazoline core structure. According to the structure of compound **7a**, a series of compound **7** were synthesized by changing the substituents R^1, R^2 and R^3 to explore the structure-activity relationship (Scheme 1).

2. Results and discussion

2.1. Chemistry

2.1.1. Synthesis of N-(substituted 4-hydroxyphenyl)-N-substituted phenylcyclopropane-1,1-dicarboxamide (5a-k)

Starting from commercially available dimethyl cyclopropane −1,1-dicarboxylate, the key intermediates N-(substituted 4-hydro- xyphenyl)-N-substituted phenylcyclopro-pane-1,1-dicarboxamides (**5**) were obtained by a simple 4-step synthesis as shown in Scheme 1, which were illustrated in detail in the previous study [20,21].

2.1.2. Synthesis of the target compounds of 7a-m

The synthesis of dihydro[1,4]dioxino[2,3-f]quinazoline derivatives (**6**) were mainly based on our previous study [19]. The compound **6** and the appropriately corresponding **5** were mixed in isopropanol in the presence of potassium carbonate to give the target compounds **7** over 60% yields (see Fig. 1).

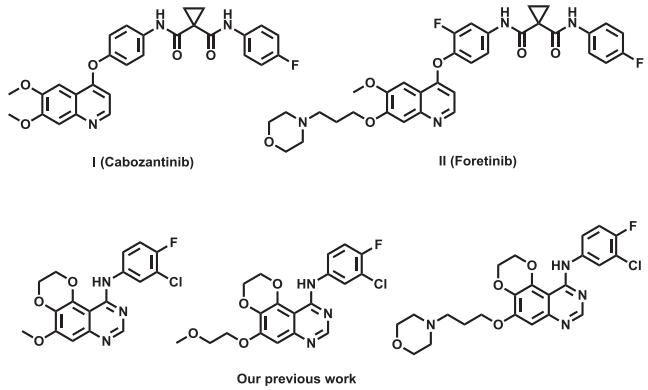

Fig. 1. The representative dual small molecule inhibitors targeting both c-Met and VEGFR-2 [Bioorg. Med. Chem. 24(2016) 3354] and our previous work targeting EGFR inhibitors based on dihydrogen[1,4] dioxin[2,3-*f*]quinazoline core.

2.2. Biological activity

2.2.1. Enzyme assay

All new compounds **(7a-m)** prepared were assayed against VEGFR-2 kinase using Kinase-Glo luminescent kinase assays. The results were shown in Table 1. Compounds **7a**, **7k**, **7l** and **7m** with good inhibitory activity against VEGFR-2 were selected to determine their inhibitory activity against c-Met. The results were summarized in Table 2. Also included was the activity of the reference drug Cabozantinib**.** Among these compounds, **7k** and **7m** showed the most potent activities with IC_{50} values of 3.5 nM and 4.8 nM against VEGFR-2, 7.3 nM and 5.8 nM against c-Met, respectively, which was comparable to Cabozantinib (IC_{50} = 3.6 nM against VEGFR-2 and 6.8 nM against c-Met).

Structure-activity relationships (SARs) were inferred from data of enzymatic experiments reported in Table 1. The type, number and position of substituents R^1 on the phenyl ring linking to the cyclopropane-1,1-dicarboxamide moiety played important roles in the enzymatic activities against VEGFR-2. The inhibitory activities of compounds **7a–g** against VEGFR-2 decreased with different single *para*-substituents in the following order: -F(**7a**) > -Cl(**7c**) > -OCH_3(**7g**) > -H(**7b**) > -Me(**7d**) > -CF_3(**7e**) ≈ -OCH(CH_3)(**7f**). The above results indicated that introduction of small electron-withdrawing

Table 1
The enzymatic inhibitory activities against VEGFR-2 for 2,3- dihydro-[1,4]dioxino [2,3-f]quinazoline derivatives.

Compd.	R^1	R^2	R^3	IC_{50} (nM)
7a	*p*-F	H	Me	18.9
7b	H	H	Me	196.7
7c	*p*-Cl	H	Me	144.8
7d	*p*-Me	H	Me	333.2
7e	*p*-CF_3	H	Me	> 1000
7f	*p*-isopropyl	H	Me	> 1000
7g	*p*-methoxy	H	Me	139.9
7h	*m*-Cl, *p*-F	H	Me	168.4
7i	*m*-F	H	Me	214.9
7j	*m*-CF_3	H	Me	834.6
7k	*p*-F	F	Me	3.5
7l	*p*-F	H	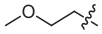	8.8
7m	*p*-F	F	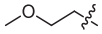	4.8
Cabozantinib				3.6

Values are averages of two independent determinations.

Table 2
The enzymatic inhibitory activities against c-Met for selected compounds.

Compd.	R^1	R^2	R^3	IC_{50} (nM)
7a	*p*-F	H	Me	18.5
7k	*p*-F	F	Me	7.3
7l	*p*-F	H	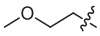	9.9
7m	*p*-F	F		5.8
Cabozantinib				6.8

Values are averages of two independent determinations.

substituents were favorable for the activities while introduction of electron-donating or strongly bulk electron-withdrawing substituents caused obvious decrease of activities.

The inhibitory activities of compounds **7a-b**, **7h-j** with different *para*-or *meta*-substituents decreased in the following order: *p*-F (**7a**) > *m*-Cl,*p*-F(**7h**) > -H(**7b**) > *m*-F(**7i**) > *m*-CF_3(**7j**). The results show that introduction of small electron-withdrawing *para*-substituent was favorable the activities while introduction of electron-withdrawing *meta* substituent caused decrease of activities. When R^1 is the ***p*-F** substituent, compound **7a**, **7k-m** showed good inhibitory activity whether R^2 were fluorine and hydrogen or R^3 were methyl and methoxyethyl. Based on the results of enzymatic inhibitory activities against VEGFR-2, compounds**7a**, **7k-m** were selected to be tested for their activity against c-Met. The results showed that methoxyethyl in R^3 and fluorine in R^2 enhanced the inhibitory activity against c-Met (Table 2).

2.2.2. Antiproliferation assay

Compounds **7a** and **7k-m** with good inhibitory activity against VEGFR-2 and c-Met were selected to evaluate their activity on a MHCC97H (liver cancer) cell line which was the c-Met dependent cell line, and a HUVEC cell line which was a VEGF-stimulated human umbilical vein endothelial cell line via a CCK-8 assay. The results were summarized in Table 3. It was clear that all the tested compounds showed better activities against HUVEC than MHCC97H. Among the tested compounds, compound **7m** with the most potent c-Met and VEGFR-2 inhibitory activities showed the most potent anticancer activities with an IC_{50} value of 15.7 nM against MHCC97H and an IC_{50} value of 0.8 nM against HUVEC, respectively, which was better than Cabozantinib.

The SARs result of antiproliferation activities was consistent with that of their inhibitory activities against c-Met and VEGFR-2, which suggested that the potent anti-cancer activities of the tested compounds were likely related to their dual c-Met and VEGFR-2 inhibitory activities.

Table 3
Cytotoxic activities of selected compounds against MHCC97H, HUVEC cell lines *in vitro*.

Compd.	MHCC97H IC_{50} (nM)	HUVEC IC_{50} (nM)
7a	234.8	–
7k	58.6	3.7
7l	80.6	6.3
7m	15.7	0.8
Cabozantinib	25.0	2.7

Values are an average of two independent determinations.
– not determined.

Table 4
Cytotoxic concentration (IC_{50}) of tested compounds.

Compd.	HEK293 IC_{50} (μM)	LO2 IC_{50} (μM)
7a	21.1	25.2
7k	15.1	12.6
7l	5.7	4.1
7m	11.9	12.2

Values are an average of two independent determinations.

2.2.3. Cytotoxicity test

The compounds **7a**, **7k-m** with good enzymatic activities against both VEGFR-2 and c-Met were evaluated for their toxicity against the HEK293 and LO2 cell lines which possessed low expression of VEGFR-2 and c-Met via a CCK8 assay. The results were summarized in Table 4. The cytotoxic concentration (IC_{50}) of **7a, 7k** and **7m** were higher than 10 μM, about two thousand times higher than IC_{50} (MHCC97H). The compounds showed low cytotoxicity against HEK293 and LO2.

2.2.4. *7k* against the xenograft tumor of MHCC97H cells in vivo

A MHCC97H cell xenograft model was established using female SCID mice (**n = 6**) to evaluate the *in vivo* anti-tumor activity effect of compound **7k**. After 2 weeks of the MHCC97H cells were subcutaneously injected into the mice to form the subcutaneous model, the drug was administered in groups. The growth curve of the tumors showed that compound **7k** had already resisted the tumor in MHCC97H cell xenograft tumor model only 8 days post treatment (Fig. 2., 60 mg/kg and Table 5**)**. Compared with the vehicle group, compound **7k** significantly inhibited the tumor growth (TGI = 120.4%) after 8 days of dosing in hepatocellular carcinoma xenograft mouse model. Moreover, from the data of body weight, the compound **7k** had no apparent toxicity during administration.

2.2.5. Docking study

In order to demonstrate anticancer activity profile of the [1,4] dioxino[2,3-*f*]quinazoline derivatives, the molecular docking simulations were performed using crystal structure of c-Met kinase (3lq8.pdb) and VEGFR-2 kinases using Discovery Studio 4.0 and Autodock 4.0. The potent compound **7m** was selected to dock into active site of c-Met kinase and VEGFR-2 kinases.

In order to predict more possible interactions of **7m** binding to c-Met and VEGFR-2 kinases, flexible docking simulations were performed based on the generated structural model as shown in Fig. 3**.** The grid size was 0.375 Å, 100 conformers were generated, cluster analyzed with 2.0 Å and energy ranked from low to high. **7m** exhibited the strong binding affinity with c-Met and VEGFR-2 kinases and found to be the most active compound from the series against MHCC97H, HUVEC, c-Met and VEGFR-2 kinases.

As shown in the 3D structure (2D structure in SI) in Fig. 3 (**A**), **7m** was docked into the binding site of c-Met kinase (**3lq8**.pdb) [3]. In the binding model, there were three hydrogen bond interactions which the protonated nitrogen atom of amide in **7m** formed a hydrogen bond with the residue of ASP1222 (O···H—N: 1.95 Å), the second nitrogen atom of

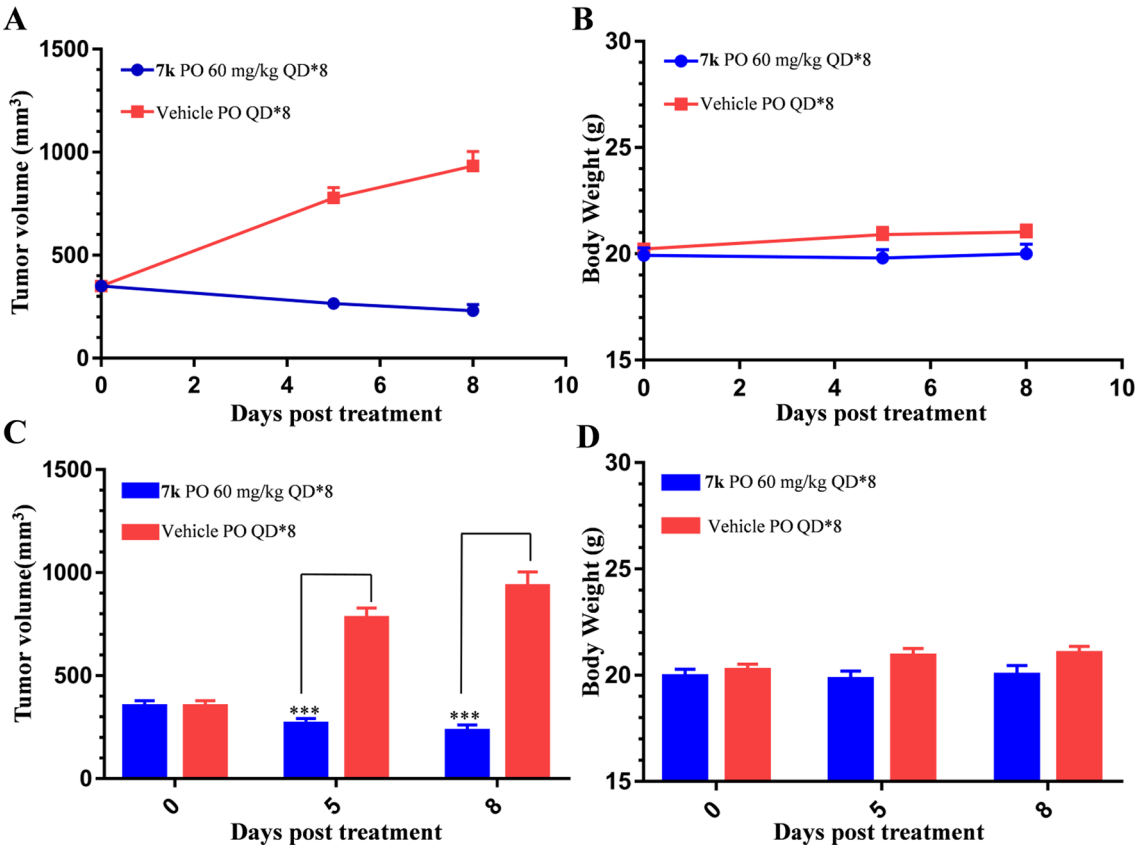

Fig. 2. (A) Growth curve of the tumors in mice following the indicated treatments (the green arrows show the time points for **7k** administration, at a dose of 60 mg/kg). (B) Body weight change of the tumor bearing mice following the indicated treatments, (C) The tumor size changes (n = 6 $^{***}p < 0.001$), (D) body weight changes (n = 6). (For interpretation of the references to colour in this figure legend, the reader is referred to the web version of this article.)

Table 5
The tumor volume TGI value on the eighth day.

	Days	Tumor volume (mm^3)	TGI (%)
Vehicle	8	933.7 ± 83.7	
7k	8	231.1 ± 40.1	120.4

quinazoline in **7m** formed a hydrogen bond with the residue of MET1160 (N···H—N: 2.07 Å) and the oxygen atom of methoxy in **7m** formed a hydrogen bond with the residue of TYR1159 (O···H—N: 2.05 Å).

Fig. 3 (**B**) showed **7m** docking into the binding site of VEGFR-2 kinase (**3u6j**.pdb) [22]. In the binding model, there were two hydrogen bond interactions. The protonated nitrogen atom of amide in **7m** formed a hydrogen bond with the residue of ASP1064 (O···H—N: 1.93 Å), the second nitrogen atom of quinazoline in **7m** formed a hydrogen bond with the residue of CYS919 (N···H—N: 1.71 Å).

The hydrogen bonds were labeled by **1**, **2**, **3**, **4** and **5** in green dotted line in Fig. 3. The docking models of **7m** binding with c-Met and VEGFR-2 kinases showed that [1,4]dioxino of **7m** occupied the receptor surface gate of the two kinases, making the binding mode more stable.

3. Conclusion

A novel series of dual c-Met and VEGFR-2 receptor tyrosine kinase inhibitors based on [1,4]dioxino[2,3-*f*]quinazoline and cyclopropane-1,1-dicarboxamide were designed and synthesized. The derivatives were obtained in good yields, and their structures were characterized by ^{1}H NMR, ^{13}C NMR and HRMS. Parts of target compounds **7a**, **7k**, **7l**

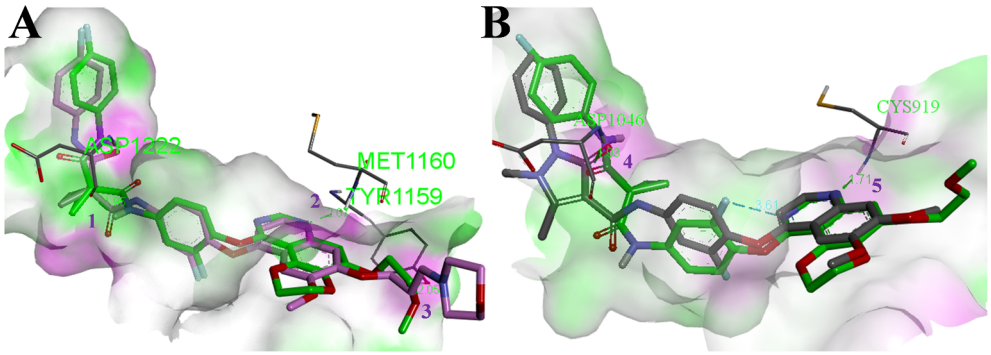

Fig. 3. 3D models of compound **7 m** (green molecular) binding into the active site of c-Met (A, **3lq8**.pdb) and VEGFR-2 (B, **3u6j**.pdb). (For interpretation of the references to colour in this figure legend, the reader is referred to the web version of this article.)

and **7m** exhibited potent inhibitory activity against c-Met and VEGFR-2 kinases with IC_{50} values lower than 20 nM. Importantly, **7m** showed even better antiproliferative activities on MHCC97H and HUVEC cells than Cabozantinib. The docking models of **7m** binding c-Met and VEGFR-2 kinases also showed that [1,4]dioxino of **7m** occupied the receptor surface gate of the two kinases, as a result the binding mode was more stable. Compound **7k** significantly inhibited the tumor growth (TGI = 120.4%) and almost no body weight changed after 8 days administration on a hepatocellular carcinoma (MHCC97H cells) xenograft mouse model. However, lots of improvements were still needed before this kind of compounds came to be a drug. For instance, target compounds maybe more stable during the metabolic process *in vivo* when the nucleus [1,4]Dioxino[2,3-*f*]quinazoline was changed to [1,4] dioxino[2,3-*f*]quinoline, and the tail R^3 of target compounds could be changed to more hydrosoluble group, such as N-(2-morpholinyl)propanyl, N-(2-dimethylethan)propanyl, N- (2-piperidine)propanyl etc. Thus further work based on these improvements was in progress.

4. Experiments

4.1. Materials and methods

The reagents were purchased and used without further purification. Melting points were determined and read on a MP120 melting point apparatus (Hanon instruments Corp., Jinan, China). The ^{1}H NMR and ^{13}C NMR spectra were measured on a Bruker 400 MHz Avance spectrometer with TMS and solvent signals allotted as internal standards. The chemical shifts are reported in ppm (δ). Splitting patterns are designed as s, singlet; d, doublet; t, triplet; m, multiplet. ESI-MS spectra were obtained on an Esquire 6000 Mass Spectrometer. HRMS data were measured using a Bruker APEX IV Fourier transform ion cyclotron resonance mass spectrometer.

4.2. General procedure for the synthesis of 1-(methoxycarbonyl) cyclopropane-1-carboxylic acid (2)

A solution of dimethyl cyclopropane-1,1-dicarboxylate (10.12 g, 63.99 mmol) in MeOH/H_2O (100 mL, 1:1 V:V), stirring in room temperature, was treated dropwise with a solution of lithium hydroxide (2.68 g, 63.99 mmol) in 20 mL H_2O. Stir for one hour after dropwise. Then adjust pH to 3 with dilute hydrochloric acid, extract with dichloromethane (50 mL) for three times, without purification go on next step.

4.3. General procedure for the synthesis of methyl 1-(phenyl- carbamoyl) cyclopropane-1-carboxylate derivatives (3a-3k)

A solution of 1-(methoxycarbonyl)cyclopropane-1- carboxylic acid (0.92 g, 6.40 mmol), aniline (0.89 g, 9.60 mmol), 3-(ethyliminomethyleneamino)-N,N-dimethyl-propan-1-amine (1.48 g, 9.6 mmol), and 1-Hydroxybenzotriazole (1.29 g, 9.6 mmol) in 20 mL dichloromethane, was stirred at room temperature for 4 h. The solvent was then removed under reduced pressure. The residue was dissolved in ethyl acetate (40 mL) and then was washed with saturated sodium carbonate (40 mL) and acid water (40 mL) successively, and dried over anhydrous sodium sulfate, evaporated to give the product (**3a-k**).

4.4. General procedure for the synthesis of N-(4-hydroxyphenyl)-N-phenylcyclopropane-1,1-dicarboxamide derivatives (5a-k)

To a solution of **3a-k** (6.40 mmol) in MeOH/H_2O (30 mL, 1:1 = V:V), lithium hydroxide (230 mg, 9.6 mmol) was added, which was stirredat room temperature for 2 h. The pH value was then adjusted to 3 with dilute hydrochloric acid, and a large amount of solid was precipitated, which was filtered and dried to give an off-white solid (**4a-k**). The next step was carried out without purification of these products. A mixture of 4a-k (1 mmol), aminophenol (1 mmol), and 3-(ethyliminomethyleneamino)-N,N- dimethyl-propan-1-amine (1 mmol) in 10 mL DMA, was stirred at room temperature for 4 h. The reaction mixture was monitored by TLC. After the starting material disappeared, the water was added and the product was extracted with ethyl acetate and the solvent was then evaporated. Finally, the product was separated by column chromatography to give a pure product (**5a-k**).

4.5. General procedure for the synthesis of N-(4-((5-methoxy-2,3- dihydro-[1,4]dioxino[2,3-f]quinazolin-10-yl)oxy)phenyl)-N-phenylcyclopropane-1,1-dicarboxamide derivatives (7a-m)

A mixture of 4-chloroquinazolines derivatives 6a-b20(1 mmol), **5a-k** (1.2 mmol) and potassium carbonate (2.4 mmol) in isopropanol (10 mL) was stirred in reflux, monitored by TLC. After the starting material disappeared, the water was added and the product was extracted with ethyl acetate. Evaporation of the solvent and separation by column chromatography give the pure product (**7a-m**).

4.5.1. methyl1-((4-fluorophenyl)carbamoyl)cyclopropane-1-carboxylate (3a)

white solid; yield: 74%; mp: 132–136 °C. ^{1}H NMR (400 MHz, DMSO-d_6, δ ppm): 10.35 (s, 1H), 7.64 (dd, J = 8.8, 5.0 Hz, 2H), 7.15 (t, J = 8.8 Hz, 2H), 3.69 (s, 3H), 1.47–1.34 (m, 4H). ESI-MS m/z calcd for $C_{12}H_{13}FNO_3$ $[M+H]^+$, 238.0; found, 238.1.

4.5.2. N-(4-fluorophenyl)-N-(4-hydroxyphenyl)cyclopropane-1,1-dicarboxamide (5a)

white solid; yield: 85%; mp: 156–159 °C. ^{1}H NMR (400 MHz, DMSO-d_6, δ ppm): 10.16 (s, 1H), 9.72 (s, 1H), 9.22 (s, 1H), 7.62 (dd, J = 8.5, 5.0 Hz, 2H), 7.35 (d, J = 8.6 Hz, 2H), 7.14 (t, J = 8.8 Hz, 2H), 6.69 (d, J = 8.7 Hz, 2H), 1.44 (s, 4H). ESI-MS m/z calcd for $C_{17}H_{16}FN_2O_3$ $[M+H]^+$, 315.1; found, 315.1.

4.5.3. N-(4-hydroxyphenyl)-N-(4-(trifluoromethyl)phenyl)cyclopropane-1,1-dicarboxamide (5j)

white solid; yield: 73%. ^{1}H NMR (400 MHz, DMSO-d_6, δ ppm): 10.28 (s, 1H), 9.88 (s, 1H), 9.34 (s, 1H), 8.13 (s, 1H), 7.83 (d, J = 8.4 Hz, 1H), 7.54 (t, J = 8.0 Hz, 1H), 7.41 (d, J = 7.8 Hz, 1H), 7.18 (s, 1H), 7.06 (t, J = 8.0 Hz, 1H), 6.99 (d, J = 8.3 Hz, 1H), 6.46 (d, J = 8.0 Hz, 1H), 1.45 (s, 4H). ESI-MS m/z calcd for $C_{18}H_{16}F_3N_2O_3$ $[M+H]^+$, 365.1; found, 365.1.

4.5.4. N-(3-chloro-4-fluorophenyl)-N-(4-hydroxyphenyl)cyclopropane-1,1-dicarboxamide (5h)

white solid; yield: 74%. ^{1}H NMR (400 MHz, DMSO-d_6, δ ppm): 10.13 (s, 1H), 9.90 (s, 1H), 9.34 (s, 1H), 7.94 (dd, J = 6.9, 2.3 Hz, 1H), 7.59–7.46 (m, 1H), 7.36 (t, J = 9.1 Hz, 1H), 7.17 (s, 1H), 7.06 (t, J = 8.0 Hz, 1H), 6.99 (d, J = 8.1 Hz, 1H), 6.46 (d, J = 7.9 Hz, 1H), 1.43 (s, 4H). ESI-MS m/z calcd for $C_{17}H_{15}ClFN_2O_3$ $[M+H]^+$, 348.1; found, 348.1.

4.5.5. N-(4-fluorophenyl)-N-(4-((5-methoxy-2,3-dihydro-[1,4]-dioxino [2,3-f]quinazolin-10-yl)oxy)phenyl)cyclopropane-1,1-dic-arboxamide (7a)

white solid; yield: 85%; mp: 242–243 °C. ^{1}H NMR (400 MHz, DMSO-d_6, δ ppm): 8.41 (s, 1H), 7.71–7.57 (m, 4H), 7.20–7.06 (m, 4H), 4.44 (d, J = 3.0 Hz, 2H), 4.38 (d, J = 2.8 Hz, 2H), 3.96 (s, 3H), 1.43 (s, 4H). ^{13}C NMR (101 MHz, DMSO-d_6, δ ppm): 168.77, 168.62, 165.36, 159.11, 156.73, 155.07, 152.30, 148.18, 147.87, 147.85, 147.84, 138.54, 132.50, 122.41, 122.34, 122.06, 121.59, 115.04, 114.82, 102.35, 100.08, 64.38, 63.49, 56.18, 40.15, 39.94, 39.73, 39.52, 39.31, 39.10, 38.89, 30.92, 15.86. HRMS (ESI) m/z calcd for $C_{28}H_{24}FN_4O_6$ $[M+H]^+$, 531.1674; found, 531.1664.

*4.5.6. N-(4-((5-methoxy-2,3-dihydro-[1,4]dioxino[2,3-f]quinaz-olin-10-yl)oxy)phenyl)-N-phenylcyclopropane-1,1-dicarboxamide (**7b**)*

white solid; yield: 78%; mp: 237–239 °C. ^{1}H NMR (400 MHz, DMSO-d_6, δ ppm): 8.41 (s, 1H), 7.67 (d, J = 8.8 Hz, 2H), 7.62 (d, J = 7.8 Hz, 2H), 7.28 (t, J = 7.8 Hz, 2H), 7.12 (d, J = 8.8 Hz, 2H), 7.02 (d, J = 9.8 Hz, 2H), 4.44 (d, J = 2.2 Hz, 2H), 4.38 (s, 2H), 3.95 (s, 3H), 1.43 (d, J = 4.0 Hz, 4H). ^{13}C NMR (101 MHz, DMSO-d_6, δ ppm): 169.07, 165.39, 155.05, 152.31, 148.17, 147.60, 138.55, 132.48, 128.49, 122.86, 121.97, 121.82, 120.47, 102.37, 100.06, 64.37, 63.50, 56.16, 30.70, 16.08. HRMS (ESI) m/z calcd for $C_{28}H_{25}N_4O_6^+$ $[M+H]^+$, 513.1769; found, 513.1756.

*4.5.7. N-(4-chlorophenyl)-N-(4-((5-methoxy-2,3-dihydro-[1,4]dioxino [2,3-f]quinazolin-10-yl)oxy)phenyl)cyclopropane-1,1-dic-arboxamide (**7c**)*

white solid; yield: 71%; mp:249–251 °C. ^{1}H NMR (400 MHz, DMSO-d_6, δ ppm): 8.42 (s, 1H), 7.65 (dd, J = 11.0, 9.0 Hz, 4H), 7.26 (d, J = 8.1 Hz, 2H), 7.11 (d, J = 8.7 Hz, 2H), 7.04 (s, 1H), 4.45 (d, J = 2.9 Hz, 2H), 4.39 (d, J = 2.4 Hz, 2H), 3.96 (s, 3H), 1.35 (s, 4H). ^{13}C NMR (101 MHz, DMSO-d_6, δ ppm): 169.27, 169.25, 165.38, 155.06, 152.32, 148.17, 147.55, 147.52, 138.55, 132.48, 128.16, 122.36, 122.05, 121.29, 102.35, 100.07, 64.36, 63.48, 56.17, 30.65, 16.20. HRMS (ESI) m/z calcd for $C_{28}H_{24}ClN_4O_6^+$ $[M+H]^+$, 547.1379; found, 547.1376

*4.5.8. N-(4-((5-methoxy-2,3-dihydro-[1,4]dioxino[2,3-f]quinazolin-10-yl)oxy)phenyl)-N-(p-tolyl)cyclopropane-1,1-dicarboxami-de (**7d**)*

white solid; yield: 73%; mp: 237–239 °C. ^{1}H NMR (400 MHz, DMSO-d_6, δ ppm): 10.11 (s, 2H), 8.40 (s, 1H), 7.68 (d, J = 8.4 Hz, 2H), 7.50 (d, J = 7.9 Hz, 2H), 7.13 (dd, J = 19.7, 8.1 Hz, 4H), 7.02 (s, 1H), 4.41 (d, J = 23.7 Hz, 4H), 3.95 (s, 3H), 2.25 (s, 3H), 1.50 (s, 4H). ^{13}C NMR (101 MHz, DMSO-d_6, δ ppm): 168.54, 168.21, 165.27, 155.08, 152.24, 148.34, 148.18, 138.51, 136.21, 136.03, 132.62, 132.50, 128.88, 122.10, 121.74, 120.60, 102.32, 100.06, 64.36, 63.48, 56.16, 40.15, 31.15, 20.43, 15.63. HRMS (ESI) m/z calcd for $C_{29}H_{27}N_4O_6^+$ $[M+H]^+$, 527.1925; found, 527.1929.

*4.5.9. N-(4-((5-methoxy-2,3-dihydro-[1,4]dioxino[2,3-f]quinazolin-10-yl)oxy)phenyl)-N-(4-(trifluoromethyl)phenyl)cyclopro-pane-1,1-dicarboxamide (**7e**)*

white solid; yield: 74%; mp: 210–213 °C. ^{1}H NMR (400 MHz, DMSO-d_6, δ ppm): 8.41 (s, 1H), 7.82 (d, J = 8.4 Hz, 2H), 7.72–7.66 (m, 2H), 7.59 (d, J = 8.5 Hz, 2H), 7.19–7.12 (m, 2H), 7.02 (s, 1H), 4.45 (d, J = 3.1 Hz, 2H), 4.39 (d, J = 2.9 Hz, 2H), 3.96 (s, 3H), 1.43 (s, 4H). 13C NMR (101 MHz, DMSO-d_6, δ ppm): 170.02, 169.53, 165.78, 155.52, 152.73, 148.66, 148.35, 139.00, 137.38, 132.96, 129.19, 126.50, 125.96, 123.81, 122.57, 121.70, 121.17, 102.82, 100.54, 64.82, 63.95, 56.61, 40.65, 40.44, 40.24, 40.03, 39.82, 39.61, 39.40, 31.48, 16.70. HRMS (ESI) m/z calcd for $C_{29}H_{24}F_3N_4O_6^+$ $[M+H]^+$, 581.1642; found, 581.1606

*4.5.10. N-(4-isopropylphenyl)-N-(4-((5-methoxy-2,3-dihydro-[1,4] dioxino[2,3-f]quinazolin-10-yl)oxy)phenyl)cyclopropane-1,1-dicarboxamide (**7f**)*

white solid; yield: 75%; mp: 235–238 °C. ^{1}H NMR (400 MHz, DMSO-d_6, δ ppm): 10.11 (s, 2H), 8.41 (s, 1H), 7.69 (d, J = 8.9 Hz, 2H), 7.53 (d, J = 8.5 Hz, 2H), 7.17 (dd, J = 8.8, 2.9 Hz, 4H), 7.02 (s, 1H), 4.48–4.42 (m, 2H), 4.38 (d, J = 2.8 Hz, 2H), 3.96 (s, 3H), 1.49 (d, J = 1.2 Hz, 4H), 1.18 (d, J = 6.9 Hz, 6H).^{13}C NMR (101 MHz, DMSO-d_6, δ ppm): 168.45, 168.13, 165.31, 155.07, 152.27, 148.30, 148.19, 143.75, 138.50, 136.57, 136.12, 132.49, 126.21, 122.16, 121.70, 120.63, 102.31, 100.08, 64.37, 63.48, 56.17, 32.91, 31.22, 23.98, 15.62. HRMS (ESI) m/z calcd for $C_{31}H_{31}N_4O_6^+$ $[M+H]^+$, 555.2238; found, 555.2230.

*4.5.11. N-(4-((5-methoxy-2,3-dihydro-[1,4]dioxino[2,3-f]quin-azolin-10-yl)oxy)phenyl)-N-(4-methoxyphenyl)cyclopropane-1,1-dicarboxamide (**7g**)*

white solid; yield: 63%; mp: 210–212 °C. ^{1}H NMR (400 MHz, DMSO-d_6, δ ppm): 10.23 (s, 1H), 9.96 (s, 1H), 8.41 (s, 1H), 7.69 (d, J = 8.9 Hz, 2H), 7.56–7.49 (m, 2H), 7.21–7.13 (m, 2H), 7.03 (s, 1H), 6.92–6.84 (m, 2H), 4.45 (dd, J = 5.3, 2.3 Hz, 2H), 4.41–4.36 (m, 2H), 3.96 (s, 3H), 3.73 (s, 3H), 1.49 (s, 4H). ^{13}C NMR (101 MHz, DMSO-d_6, δ ppm): 168.89, 168.61, 165.76, 156.06, 155.54, 152.73, 148.74, 148.66, 138.98, 136.58, 132.97, 132.27, 122.77, 122.59, 122.08, 114.09, 102.79, 100.55, 64.83, 63.95, 56.64, 55.65, 40.64, 40.43, 40.22, 40.01, 39.81, 39.60, 39.39, 31.52, 16.05. HRMS (ESI) m/z calcd for $C_{29}H_{27}N_4O_7^+$, $[M+H]^+$, 543.1874; found, 543.1871.

*4.5.12. N-(3-chloro-4-fluorophenyl)-N-(4-((5-methoxy-2,3-dih-ydro-[1,4]dioxino[2,3-f]quinazolin-10-yl)oxy)phenyl)cyclopro-pane-1,1-dicarboxamide (**7h**)*

white solid; yield: 69%; mp: 235–238 °C. ^{1}H NMR (400 MHz, DMSO-d_6, δ ppm): 10.22 (d, J = 43.1 Hz, 2H), 8.41 (s, 1H), 7.98 (dd, J = 6.9, 2.3 Hz, 1H), 7.69 (d, J = 8.8 Hz, 2H), 7.57 (d, J = 7.5 Hz, 1H), 7.36 (t, J = 9.0 Hz, 1H), 7.15 (d, J = 8.9 Hz, 2H), 7.04 (s, 1H), 4.45 (d, J = 2.4 Hz, 2H), 4.38 (d, J = 1.9 Hz, 2H), 3.96 (s, 3H), 1.48 (s, 4H). ^{13}C NMR (101 MHz, DMSO-d_6, δ ppm): 168.50, 168.21, 165.04, 155.18, 152.70, 152.33, 148.26, 140.29, 138.53, 132.58, 129.41, 122.09, 120.87, 120.80, 118.91, 118.73, 117.24, 117.07, 116.67, 116.46, 113.99, 102.36, 100.08, 64.40, 63.53, 56.21, 31.85, 15.53. HRMS (ESI) m/z calcd for $C_{28}H_23ClFN_4O_6^+$ $[M+H]^+$, 565.1285; found, 565.1281.

*4.5.13. N-(3-fluoro-4-((5-methoxy-2,3-dihydro-[1,4]dioxino[2,3-f] quinazolin-10-yl)oxy)phenyl)-N-(3-fluorophenyl)cyclopropane-1,1-dicarboxamide (**7i**)*

white solid; yield: 73%; mp: 231–237 °C. ^{1}H NMR (400 MHz, DMSO-d_6, δ ppm): ^{1}H NMR (400 MHz, DMSO) δ 10.32 (s, 2H), 8.41 (s, 1H), 7.75–7.58 (m, 3H), 7.45–7.27 (m, 2H), 7.16 (d, J = 8.9 Hz, 2H), 7.03 (s, 1H), 6.88 (td, J = 8.3, 1.9 Hz, 1H), 4.48–4.42 (m, 2H), 4.38 (d, J = 2.8 Hz, 2H), 3.96 (s, 3H), 1.48 (d, J = 3.7 Hz, 4H). ^{13}C NMR (101 MHz, DMSO-d_6, δ ppm): 169.01, 168.73, 165.76, 163.70, 161.30, 155.54, 152.73, 148.73, 148.65, 138.98, 136.71, 132.96, 130.52, 130.42, 122.57, 122.16, 116.53, 115.33, 110.30, 110.09, 107.72, 107.46, 102.79, 100.55, 64.83, 63.95, 56.64, 40.63, 40.42, 40.21, 40.00, 39.79, 39.58, 39.38, 32.16, 16.02. HRMS (ESI) m/z calcd for $C_{28}H_{24}FN_4O_6^+$ $[M+H]^+$, 531.1674; found, 531.1674.

*4.5.14. N-(3-fluoro-4-((5-methoxy-2,3-dihydro-[1,4]dioxino [2,3-f] quinazolin-10-yl)oxy)phenyl)-N-(3-(trifluoromethyl)phenyl)cyclopropane-1,1-dicarboxamide (**7j**)*

white solid; yield: 78%; mp: 239–242 °C. ^{1}H NMR (400 MHz, DMSO-d_6, δ ppm): 10.40 (s, 2H), 8.44 (s, 1H), 8.15 (s, 1H), 7.83 (d, J = 8.1 Hz, 1H), 7.63 (t, J = 2.0 Hz, 1H), 7.51 (dd, J = 17.9, 9.4 Hz, 2H), 7.43–7.33 (m, 2H), 7.03 (s, 1H), 6.94 (dd, J = 8.0, 1.6 Hz, 1H), 4.48–4.41 (m, 2H), 4.42–4.29 (m, 2H), 3.96 (s, 3H), 1.46 (s, 4H). ^{13}C NMR (101 MHz, DMSO-d_6, δ ppm): 168.70, 168.24, 165.00, 155.13, 152.68, 152.30, 148.23, 140.42, 138.49, 132.53, 129.58, 129.34, 129.02, 128.26, 125.56, 123.93, 122.85, 120.14, 119.54, 119.50, 119.47, 119.44, 117.12, 117.01, 116.64, 116.60, 113.95, 102.32, 100.06, 64.36, 63.48, 56.16, 40.15, 39.94, 39.73, 39.52, 39.31, 39.10, 38.89, 31.94, 15.53. HRMS (ESI) m/z calcd for $C_{29}H_{24}F_3N_4O_6^+$ $[M+H]^+$, 581.1642; found, 581.1649.

*4.5.15. N-(3-fluoro-4-((5-methoxy-2,3-dihydro-[1,4]dioxino [2,3-f] quinazolin-10-yl)oxy)phenyl)-N-(4-fluorophenyl)cyclopropane-1,1-dicarboxamide (**7k**)*

white solid; yield: 89%; mp: 239–242 °C. ^{1}H NMR (400 MHz, DMSO-d_6, δ ppm): 10.33 (s, 1H), 10.05 (s, 1H), 8.44 (s, 1H), 7.80 (d, J = 13.0 Hz, 1H), 7.70–7.59 (m, 2H), 7.45 (d, J = 8.9 Hz, 1H), 7.33 (t, J = 8.8 Hz, 1H), 7.15 (t, J = 8.9 Hz, 2H), 7.07 (s, 1H), 4.47 (d,

J = 2.6 Hz, 2H), 4.40 (d, J = 2.6 Hz, 2H), 3.97 (s, 3H), 1.48 (s, 4H).^{13}C NMR (101 MHz, DMSO-d_6, δ ppm): 168.78, 168.47, 164.75, 159.99, 157.60, 155.80, 154.88, 152.58, 152.45, 148.72, 138.84, 138.11, 138.02, 135.63, 135.61, 135.48, 135.35, 133.20, 124.36, 123.01, 122.93, 116.97, 116.95, 115.58, 115.36, 109.21, 108.98, 102.22, 100.62, 64.88, 64.00, 56.70, 40.64, 40.43, 40.22, 40.01, 39.80, 39.60, 39.39, 32.18, 15.88. HRMS (ESI) *m/z* calcd for $C_{28}H_{23}F_2N_4O_6^+$ [M + H]$^+$, 549.1580; found, 549.1586.

4.5.16. N-(4-fluorophenyl)-N-(4-((5-(2-methoxyethoxy)-2,3-dihydro-[1,4]dioxino[2,3-f]quinazolin-10-yl)oxy)phenyl)cyclopropane-1,1-dicarboxamide (7l)

white solid; yield: 81%; mp: 245–248 °C. ^{1}H NMR (400 MHz, DMSO-d_6, δ ppm): 10.11 (d, J = 11.8 Hz, 2H), 8.40 (s, 1H), 7.72–7.62 (m, 4H), 7.20–7.10 (m, 4H), 7.03 (s, 1H), 4.45 (d, J = 4.4 Hz, 2H), 4.40 (d, J = 3.7 Hz, 2H), 4.33–4.25 (m, 2H), 3.78–3.71 (m, 2H), 3.35 (s, 3H), 1.49 (s, 4H). HRMS (ESI) *m/z* calcd for $C_{30}H_{28}FN_4O_7^+$ [M + H]$^+$, 575.1937; found, 575.1918.

4.5.17. N-(3-fluoro-4-((5-(2-methoxyethoxy)-2,3-dihydro-[1,4]dioxino[2,3-f]quinazolin-10-yl)oxy)phenyl)-N-(4-fluorophenyl)cyclopropane-1,1-dicarboxamide (7m)

white solid; yield: 81%; mp: 237–240 °C. ^{1}H NMR (400 MHz, DMSO-d_6, δ ppm): 10.31 (s, 1H), 10.04 (s, 1H), 8.43 (s, 1H), 7.80 (dd, J = 12.9, 1.9 Hz, 1H), 7.65 (dd, J = 8.9, 5.1 Hz, 2H), 7.46 (d, J = 8.7 Hz, 1H), 7.33 (t, J = 8.8 Hz, 1H), 7.15 (t, J = 8.9 Hz, 2H), 7.08 (s, 1H), 4.47 (d, J = 3.1 Hz, 2H), 4.41 (d, J = 2.2 Hz, 2H), 4.35–4.26 (m, 2H), 3.80–3.68 (m, 2H), 3.35 (s, 3H), 1.48 (s, 4H). ^{13}C NMR (101 MHz, DMSO-d_6, δ ppm): 168.76, 168.46, 164.73, 159.98, 157.59, 155.00, 154.88, 152.56, 152.46, 148.64, 138.93, 138.14, 138.04, 135.66, 135.63, 135.48, 135.35, 133.22, 124.37, 122.99, 122.92, 116.96, 116.94, 115.58, 115.36, 109.20, 108.97, 102.23, 101.23, 70.49, 68.69, 64.86, 63.98, 58.69, 32.19, 15.87. HRMS (ESI) *m/z* calcd for $C_{30}H_{27}F_2N_4O_7^+$ [M + H]$^+$, 593.1842; found, 593.1848.

4.6. VEGFR-2 and c-Met inhibitory assay

Prepare all the solutions using autoclaved, deionized water and analytical grade reagents. Prepare and store all the reagents at room temperature (unless indicated otherwise).

EDTA solution (0.5 M, pH 8.0): add 95 mL ultra-pure water to 14.612 g EDTA, adjust the pH to 8.0 using NaOH solution, add 5 mL ultra-pure water;

1 × Kinase Assay Buffer: add 25 mL HEPES solution (1 M), 190.175 mg EGTA, 5 mL $MgCl_2$ solution (1 M), 1 mL DTT, 50 μL tween-20, 450 mL ultrapure water, adjust pH to 7.5 and constant volume to 500 mL using ultrapure water;

4 × Stop solution (40 mM): Mix 0.8 mL of the foregoing EDTA solution, 1 mL 10 × Detection Buffer and 8.2 mL ultra-pure water;

1 × Detection Buffer: Mix 1 mL 10 × Detection Buffer with 9 mL water;

4 × VEGFR Kinase solution (1.74 nM, 521 times diluted, stored on ice): 1.2 μL VEGFR or c-Met Kinase mother liquor (0.909 μM) was added to 624 μL 1 × Kinase Assay Buffer and mixed;

4 × ULight™-labeled JAK1 (substrate) (200 nM, 25 times diluted): 24 μL ULight™-labeled JAK1 (mother liquor concentration 5 μM) was added to 576 μL 1 × Kinase Assay Buffer and mixed;

4 × ATP Solution (40 μM, 250 times diluted): add 3 μL ATP solution (10 mM) to 747 μL 1 × Kinase Assay Buffer and mixed;

4 × Detection Mix (8 nM, 390.6 times diluted): 3 μL Europium- anti-phospho-tyrosine antibody (PT66) (3.125 μM) was added to 1169 μL 1 × Detection Buffer and mixed;

2 × substrate/ATP Mix: 560 μL foregoing 4 × ULight™-labeled JAK1 and 560 μL 4 × ATP solution and mixed (prepared before use).

The assays used an ULight-labeled peptide substrate and an Europium-W1024-labeled antiphosphotyrosine antibody. The VEGFR-2 and c-Met kinase was purchased from Carna Biosciences, Inc. (New York, USA). The 384-well plates were obtained from PerkinElmer. Compounds were dissolved in DMSO and diluted to 11 concentrations at a tripling rate from 2.500 μM to 0.042 nM and added 2.5 μL to 384-well plates. 5 μL 2 × VEGFR-2 kinase solution (0.5 nM) was added to 384-well plates homogeneous mixing and pre-reaction at room temperature for 30 min. Next, 2.5 μL 4 × Ultra ULightTM-JAK-1(Tyr1023) Peptide (200 nM)/ATP (40 μM) was added to the corresponding wells of a 384-well plate. Negative control: 2.5 μL/well 4 × substrate/ATP mixture and 7.5 μL 1 × kinase assay buffer in 384-well plate well. Positive control: 2.5 μL/well 4 × substrate/ATP mixture, 2.5 μL/well 1 × kinase assay buffer with 16% DMSO, 5 μL/well 2 × VEGFR-2 kinase solution were added to the 384-well plate, The final concentration of DMSO in the mixing system was 4%.

After incubation at room temperature and dark for 60 min, 5 μL 4 × stop solution was added to corresponding wells to react for 5 min and then 5 μL 4 × detection mix was added to the corresponding wells of a 384-well plate. The mixture was centrifugally mixed and stayed for 60 min at room temperature for colour development. The plate was read using a Envision plate reader. The inhibition rate (%) = (positive well reading-compound well reading)/(positive well reading-negative well reading) × 100. The corresponding IC_{50} values were calculated using GraphPad Prism 5.0.

4.7. Cell proliferative assay

The antiproliferative activity was determined using cell-counting kit-8 assay (Dojindo, Japan). MHCC97H cells were seeded at a density of 6×10^3 cells /well in 96-well plates and were incubated at 37 Centigrade overnight in a humidified incubator containing 5% CO_2. Cells were dosed with compounds at a final concentration ranging from 0.025 μM to 80 μM in each well. After 48 h, 10 μL of the CCK-8 solution was added and incubated for 1 to4 h. Cell survival was determined by measuring the absorbance at 470 nm using a microplate reader. A calibration curve was obtained by using the data from the wells that contain known numbers of viable cells.

4.8. Antitumor activity of 7k on the xenograft tumor of MHCC97H cells

In vivo animal experimental protocol was approved by the animal ethics committee of Beijing Scitech-MQ Pharmaceuticals Limited. Six-week-old female nude mice (BALB/c) were housed at six mice per cage in a specific pathogen-free room with a 12 h light/dark schedule at 25 °C ± 1 °C and were fed with an autoclaved chow diet and water ad libitum. The mice were randomly divided into indicated groups (6 mice/group) before tumor cell inoculation, and a double-blinded evaluation was performed when measuring tumor weight as well as tumor volume. MHCC97H cells were subcutaneously injected into the right back of the mice (1.0×10^7 cells/mouse) to get the subcutaneous model. When the tumors reached 300–400 mm^3, the drug was administered in groups. The animals were weighed before administration, and the tumor volume was measured. Vehicle and **7k** were given orally once a day for 8 days. The body weight and the tumor volume were measured every three days. The growth curve of the tumor was calculated according to the formula: $V = 0.5\ a \times b^2$. Tumor growth inhibition (TGI) was calculated using the following formula: TGI (%) = $[1-(T - T_0)/(C - C_0)] \times 100$, where T and T_0 were the mean tumor weight on a specific experimental day and on the first day of administration group, likewise, where C and C_0 were the mean tumor weight for the vehicle group.

4.9. Docking study

Compound **7m** docked into the c-Met and VEGFR-2 complex structure (PDB code: **3lq8**.pdb and **3u6j**.pdb, downloaded from the PDB bank). Ligands and unwanted water were removed and **7m** was

drawn and optimized by DS4.0. Docking procedure was performed by AutoDock 4.0. The grid size was 0.375 Å, 100 conformers being generated, energy ranking through low to high. After docking finished, only one best docking conformation was exported.

Acknowledgments

The authors would like to acknowledge financial support from Beijing Key Laboratory of Environmental & Viral Oncology, Beijing Scitech-MQ Pharmaceuticals Limited STTG002 project funds and development funds and Beijing Key Laboratory for Green Catalysis and Separation.

Conflict of interest

The authors declare no conflict of interest.

Appendix A. Supplementary material

Supplementary data to this article can be found online at https://doi.org/10.1016/j.bioorg.2019.04.010.

References:

[1] M.A. Feitelsona, A. Arzumanyan, R.J. Kulathinal, S.W. Blain, R.F. Holcombe, J. Mahajna, M. Marino, M.L. Martinez-Chantar, R. Nawroth, I. Sanchez-Garcia, D. Sharma, N.K. Saxena, N. Singh, P.J. Vlachostergios, S. Guom, K. Honoki, H. Fujii, A.G. Georgakilas, A. Bilsland, A. Amedei, E. Niccolai, A. Amin, S.S. Ashraf, C.S. Boosani, G. Guha, M.R. Ciriolo, K. Aquilano, S. Chen, S.I. Mohammed, Sustained proliferation in cancer: Mechanisms and novel therapeutic targets, Semin. Cancer Biol. 35 (2015) S25–S54.

[2] F.M. Yakes, J. Chen, J. Tan, K. Yamaguchi, Y.C. Shi, P.W. Yu, F. Qian, F.L. Chu, F. Bentzien, B. Cancilla, J. Orf, A. You, A.D. Laird, S. Engst, L. Lee, J. Lesch, Y.C. Chou, A.H. Joly, Cabozantinib (XL184), a novel MET and VEGFR2 inhibitor, simultaneously suppresses metastasis, angiogenesis, and tumor growth, Mol. Cancer Ther. 10 (2011) 2298–2308.

[3] F. Qian, S. Engst, K. Yamaguchi, P.W. Yu, K.A. Won, L. Mock, T. Lou, J. Tan, C. Li, D. Tam, J. Lougheed, F.M. Yakes, F. Bentzien, W. Xu, T. Zaks, R. Wooster, J. Greshock, A.H. Joly, Inhibition of tumor cell growth, invasion, and metastasis by EXEL-2880 (XL880, GSK1363089), a novel inhibitor of HGF and VEGF receptor tyrosine kinases, Cancer Res. 69 (2009) 8009–8016.

[4] J. Zhang, X. Jiang, Y. Jiang, M. Guo, S. Zhang, J. Li, J. He, J. Liu, J. Wang, L. Ouyang, Recent advances in the development of dual VEGFR and c-Met small molecule inhibitors as anticancer drugs, Eur. J. Med. Chem. 108 (2016) 495–504.

[5] C. Birchmeier, W. Birchmeier, E. Gherardi, G.F. Vande Woude, Met, metastasis, motility and more, Nat. Rev. Mol. Cell Biol. 4 (2003) 915–925.

[6] P.M. Comoglio, S. Giordano, L. Trusolino, Drug development of MET inhibitors: targeting oncogene addiction and expedience, Nat. Rev. Drug Discovery 7 (2008) 504–516.

[7] Y. Liao, R. Grobholz, U. Abel, L. Trojan, M.S. Michel, P. Angel, D. Mayer, Int. J. Cancer 107 (2003) 676–680.

[8] F. Cappuzzo, A. Marchetti, M. Skokan, E. Rossi, S. Gajapathy, L. Felicioni, M.D. Grammastro, M.G. Sciarrotta, F. Buttitta, M. Incarbone, Increased MET gene copy number negatively affects survival of surgically resectednon-small-cell lung cancer patients, J. Clin. Oncol. 27 (2009) 1667–1674.

[9] J.G. Christensen, J. Burrows, R. Salgia, c-Met as a target for human cancer and characterization of inhibitors for therapeutic intervention, Cancer Lett. 225 (2005) 1–26.

[10] K. Holmes, O.L. Roberts, A.M. Thomas, M.J. Cross, Vascular endothelial growth factor receptor-2: Structure, function, intracellular signalling and therapeutic inhibition, Cell. Signal. 19 (2007) 2003–2012, https://doi.org/10.1016/j.cellsig.2007.05.013.

[11] J. Gille, R. Heidenreich, A. Pinter, J. Schmitz, B. Boehme, D.J. Hicklin, R. Henschler, G. Breier, Simultaneous blockade of VEGFR-1 and VEGFR-2 activation is necessary to efficiently inhibit experimental melanoma growth and metastasis formation, Int. J. Cancer 120 (2007) 1899–1908.

[12] N. Ferrara, H.P. Gerber, J.L. Couter, Nat. Med. 9 (2003) 669–676.

[13] M. Mannion, S. Raeppel, S. Claridge, N. Zhou, O. Saavedra, L. Isakovic, L. Zhan, F. Gaudette, F. Raeppel, R. Déziel, N. Beaulieu, H. Nguyen, I. Chute, C. Beaulieu, I. Dupont, M.F. Robert, S. Lefebvre, M. Dubay, J. Rahil, J. Wang, H.S. Croix, A.R. Macleod, J.M. Besterman, A. Vaisburg, *N*-(4-(6,7-Disubstituted-quinolin-4-yloxy)-3-fluorophenyl)-2-oxo-3-phenylimidazolidine-1-carboxamides: a novel series of dual c-Met/VEGFR2 receptor tyrosine kinase inhibitors, Bioorganic Med. Chem. Lett. 19 (2009) 6552–6556.

[14] S. Claridge, F. Raeppel, M.C. Granger, N. Bernstein, O. Saavedra, L. Zhan, D. Llewellyn, A. Wahhab, R. Deziel, J. Rahil, N. Beaulieu, H. Nguyen, I. Dupont, A. Barsalou, C. Beaulieu, I. Chute, S. Gravel, M.F. Robert, S. Lefebvre, M. Dubay, R. Pascal, J. Gillespie, Z. Jin, J. Wang, J.M. Besterman, A.R. MacLeodb, A. Vaisburga, Discovery of a novel and potent series of thieno[3,2-b]pyridine-based inhibitors of c-Met and VEGFR2 tyrosine kinases, Bioorganic Med. Chem. Lett. 18 (2008) 2793–2798.

[15] B. Bilanges, N. Torbett, B. Vanhaesebroeck, Killing two kinase families with one stone, Nat. Chem. Biol. 4 (2008) 648–649.

[16] O. Saavedra, S. Claridge, L. Zhan, F. Raeppel, M.C. Granger, S. Raeppel, M. Mannion, F. Gaudette, N. Zhou, L. Isakovic, N3-Arylmalonamides: a new series of thieno[3,2-b]pyridine based inhibitors of c-Met and VEGFR2 tyrosine kinases, Bioorganic Med. Chem. Lett. 19 (2009) 6836–6839.

[17] Y. Fujiwara, A. Miwa, K. Nakamura, T. Nishitoba, T. Osawa, T. Senga, PCT Int. Appl. WO2003000660, 2003.

[18] M. Zillhardt, S.M. Park, I.L. Romero, K. Sawada, A. Montag, T. Krausz, S.D. Yamada, M.E. Peter, E. Lengyel, Foretinib (GSK1363089), an orally available multikinase inhibitor of c-Met and VEGFR-2, blocks proliferation, induces anoikis, and impairs ovarian cancer metastasis, Clin. Cancer Res. 17 (2011) 4042–4051.

[19] X. Qin, Z. Li, L. Yang, P. Liu, L. Hu, C. Zeng, Z. Pan, Discovery of new [1,4]dioxino [2,3-f]quinazoline-based inhibitors of EGFR including the T790M/L858R mutant, Bioorg. Med. Chem. 24 (2016) 2871–2881.

[20] Y. Long, M. Geng, Z. Xu, J. Ai PCT Int. Appl. WO2016184434, 2016.

[21] Q. Zhang, H. Zhang, L. Yang, H. Yang, L. Zhou, S. Yu, N Zheng, Z. Xu, C. Hu, PCT Int. Appl. WO2018153293, 2018.

[22] M.H. Norman, L. Liu, M. Lee, N. Xi, I. Fellows, N.D. D'Angelo, C. Dominguez, K. Rex, S.F. Bellon, T.S. Kim, I. Dussault, Structure-based design of novel class II c-Met inhibitors: 1. Identification of pyrazolone- based derivatives, J. Med. Chem. 55 (2012) 1858–1867.